# Global Effects of the Energetics of Coenzyme Binding: NADPH Controls the Protein Interaction Properties of Human Cytochrome P450 Reductase†

Alex Grunau,‡ Mark J. Paine,§ John E. Ladbury,|| and Aldo Gutierrez*,‡

*Department of Biochemistry, University of Leicester, The Henry Wellcome Building, Lancaster Road, Leicester LE1 9HN, U.K., Biomedical Research Centre, University of Dundee, Ninewells Hospital and Medical School, Dundee DD1 9SY, U.K., and Department of Biochemistry and Molecular Biology, University College London, Gower Street, London WC1E 6BT, U.K.*

*Received October 17, 2005; Revised Manuscript Received November 29, 2005*

ABSTRACT: The thermodynamics of coenzyme binding to human cytochrome P450 reductase (CPR) and its isolated FAD-binding domain have been studied by isothermal titration calorimetry. Binding of 2′,5′-ADP, $NADP^+$, and $H_4NADP$, an isosteric NADPH analogue, is described in terms of the dissociation binding constant ($K_d$), the enthalpy ($\Delta H_B$) and entropy ($T\Delta S_B$) of binding, and the heat capacity change ($\Delta C_p$). This systematic approach allowed the effect of coenzyme redox state on binding to CPR to be determined. The recognition and stability of the coenzyme−CPR complex are largely determined by interaction with the adenosine moiety ($K_{d2',5'-ADP} = 76$ nM), regardless of the redox state of the nicotinamide moiety. Similar heat capacity change ($\Delta C_p$) values for 2′,5′-ADP (−210 cal $mol^{-1}$ $K^{-1}$), $NADP^+$ (−230 cal $mol^{-1}$ $K^{-1}$), and $H_4NADP$ (−220 cal $mol^{-1}$ $K^{-1}$) indicate no significant contribution from the nicotinamide moiety to the binding interaction surface. The coenzyme binding stoichiometry to CPR is 1:1. This result validates a recently proposed one-site kinetic model [Daff, S. (2004) *Biochemistry 43*, 3929−3932] as opposed to a two-site model previously suggested by us [Gutierrez, A., Lian, L.-Y., Wolf, C. R., Scrutton, N. S., and Roberts, C. G. K. (2001) *Biochemistry 40*, 1964−1975]. Calorimetric studies in which binding of 2′,5′-ADP to CPR ($T\Delta S_B = -13400 \pm 200$ cal $mol^{-1}$, 35 °C) was compared with binding of the same ligand to the isolated FAD-binding domain ($T\Delta S_B = -11200 \pm 300$ cal $mol^{-1}$, 35 °C) indicate that the number of accessible conformational substates of the protein increases upon 2′,5′-ADP binding in the presence of the FMN-binding domain. This pattern was consistently observed along the temperature range that was studied (5−35 °C). This contribution of coenzyme binding energy to domain dynamics in CPR agrees with conclusions from previous temperature-jump studies [Gutierrez, A., Paine, M., Wolf, C. R., Scrutton, N. S., and Roberts, G. C. K. (2002) *Biochemistry 41*, 4626−4637]. A combination of calorimetry and stopped-flow spectrophotometry kinetics experiments showed that this linkage between coenzyme binding energetics and diffusional domain motion impinges directly on the molecular recognition of cytochrome *c* by CPR. Single-turnover reduction of cytochrome *c* by CPR ($k_{max} = 15$ $s^{-1}$, $K_d = 37$ $\mu$M) is critically coupled to coenzyme binding through ligand-induced motions that enable the FMN-binding domain to overcome a kinetically unproductive conformation. This is remarkable since the FMN-binding domain is not directly involved in coenzyme binding, the NADP(H) binding site being fully contained in the FAD-binding domain. Sequential rapid mixing measurements indicate that harnessing of coenzyme binding energy to the formation of a kinetically productive CPR−cytochrome *c* complex is a highly synchronized event. The inferred half-time for the decay of this productive conformation ($\tau_{50}$) is 330 ± 70 ms only. Previously proposed structural and kinetic models are discussed in light of these findings.

Cytochrome P450 enzymes play a crucial role in the metabolism of endogenous compounds in the endoplasmic reticulum. Detoxification reactions catalyzed by these enzymes are critically dependent on electron transfer from the cytochrome P450 reductase enzyme (CPR,[1] EC 1.6.2.4). CPR is a versatile enzyme that can also transfer electrons to other redox proteins such as cytochrome *c* (*1*), cytochrome $b_5$ (*2*), heme oxygenase (*3*), and the fatty acid elongation system (*4*). Recently, CPR has been found to carry out in vivo reductive activation of anticancer prodrugs in a hypoxia-specific manner, resulting in a markedly cytotoxic effect on cancer tumors (*5*, *6*). Thus, this enzyme has also become a target for novel anticancer therapy (*7*, *8*).

† This work was funded by the Wellcome Trust. A. Gutierrez is a Wellcome Trust Career Development Research Fellow (069246). J.E.L. is a Wellcome Trust Senior Research Fellow.

* To whom correspondence should be addressed. E-mail: afg2@le.ac.uk. Telephone: (+44) 0116 229 7102. Fax: (+44) 0116 229 7018.

‡ University of Leicester.

§ University of Dundee.

|| University College London.

[1] Abbreviations: CPR, cytochrome P450 reductase; 2′,5′-ADP, adenosine 2′,5′-diphosphate; 3′,5′-ADP, adenosine 3′,5′-diphosphate; $NADP^+$, $\beta$-nicotinamide adenine dinucleotide phosphate, oxidized form; $H_4NADP$, 1,4,5,6-tetrahydro-NADP; NADPH, $\beta$-nicotinamide adenine dinucleotide phosphate, reduced form; $NMN^+$, nicotinamide mononucleotide, oxidized form; FMN, flavin mononucleotide; FAD, flavin adenine dinucleotide; P450-$BM_3$, cytochrome P450 (CYP102), isolated from *Bacillus megaterium*; NOS, nitric oxide synthase.

10.1021/bi052115r CCC: $33.50 
Published on Web 01/10/2006

Biological electron transfer is carried out by redox proteins associated in large, dynamic complexes. Often, a single protein comprises several redox centers, each bound to a structurally independent domain. CPR is a complex multidomain protein. It contains two flavin-binding domains containing redox centers: an FAD-binding domain and an FMN-binding domain. A so-called "linker domain", present as an insert in the sequence of the FAD-binding domain, interacts structurally with both the other domains and may be involved in determining their mutual orientation, the FMN-binding domain being connected to the FAD-binding domain through a highly flexible "hinge". NADPH, the physiological substrate, binds to a well-defined Rossmann fold contained in the FAD-binding domain (Figure 1). Each flavin-binding domain is an independent folding unit, reflecting the fact that they have evolved from separate proteins. The FAD-binding domain is related to the ferredoxin $NADP^+$ reductase (FNR) family of enzymes, while the FMN-binding domain is phylogenetically related to the flavodoxins (*9*).

Human CPR has been the object of extensive kinetic studies in recent years (for a review, see ref *10*). Of particular relevance to the work presented here is evidence that the binding of adenosine phosphates, 2′,5′-ADP or 2′-AMP, affects internal electron transfer in this enzyme. Temperature-jump studies have shown that interdomain electron transfer in CPR (from FAD to FMN) is severely gated by domain motion (*11*). Further equilibrium-perturbation studies established that binding of 2′,5′-ADP or 2′-AMP increases the observed interdomain electron-transfer rate several fold (*12*). Early studies by Murataliev and Feyeresien suggested a functional role for NADP(H) binding in regulating flavin redox properties during the catalytic turnover of P450-$BM_3$, a member of the CPR family (*13*, *14*). Recent work on nitric oxide syntase (NOS), another CPR homologue, has established a critical role for coenzyme binding in the control mechanisms operating in that enzyme (*15*). Therefore, the search for the molecular basis for this interplay between coenzyme binding and electron transfer in this protein family has now become the object of intensive work by several groups (for a review, see ref *16*).

Determination of the different energetic contributions to binding interaction enables the linkage between ligand binding and protein function to be studied in terms of molecular driving forces (*17*). We have applied isothermal titration calorimetry (ITC) to study the energetics of coenzyme binding to the CPR enzyme and its isolated FAD-binding domain. This analysis has been further extended to the study of the interaction between this enzyme and cytochrome *c* through the use of a combination of fast kinetics and microcalorimetry. We demonstrate that binding of NADPH to the FAD-binding domain actually modulates the interaction of CPR with cytochrome *c* by affecting the dynamics of a different domain, the distal FMN-binding domain. These results reveal that coenzyme binding energy has a global effect on the entire CPR protein.

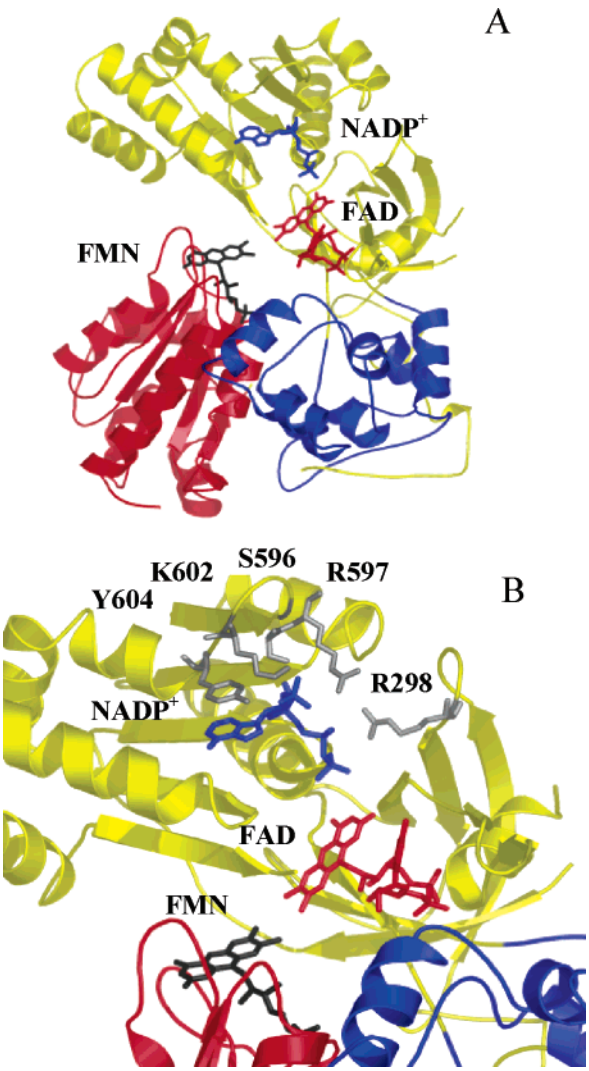


FIGURE 1: Crystal structure of $NADP^+$-bound rat CPR in its oxidized form (*30*). (A) Overall polypeptide fold. The different structural domains are indicated: FAD-binding domain (yellow), linker "hinge" domain (blue), and FMN-binding domain (red). The crystal structure shows only a $NADP^+$ coenzyme molecule (blue) bound to the FAD-binding domain. The two flavin cofactors, FAD (red) and FMN (black), are separated by only 4 Å. This structure is likely to represent a transient intermediate in the electron-transfer cycle, and the observed internal electron-transfer rate is several orders of magnitude lower than the intrinsic rate predicted from this conformation (*11*). (B) Coenzyme-binding site. The main residues known to interact with the adenosine moiety are shown (R298, S596, R597, K602, and Y604). The nicotinamide moiety of $NADP^+$ is highly disordered in the crystal. This figure was created using PyMOL Molecular Graphics System (DeLano Scientific LLC).

## EXPERIMENTAL PROCEDURES

*Materials.* NADPH, $NADP^+$, and 2′,5′-ADP were purchased from Sigma. All other chemicals were analytical grade. Glucose-6-phosphate dehydrogenase, horse heart cytochrome *c*, and bovine serum albumin (BSA) were obtained from Sigma. High-purity hydrogen (99.995% minimum) for $H_4NADP$ synthesis was supplied by BOC (Surrey, U.K.). Palladium (10% on activated charcoal) was purchased from ACROS Organics.

*Protein Purification and Sample Preparation.* Human fibroblast CPR (lacking the N-terminal membrane-anchoring region) and the functional FAD-binding domain were expressed in *Escherichia coli* BL21(DE3)pLysS from appropriate pET15b plasmid constructs. The FAD-binding domain construct that was used includes the "linker" domain (*18*). The R597A mutant was constructed following standard mutagenesis protocols.

Proteins were purified as described previously (*18*, *19*) with the notable exception of the omission of the 2′,5′-ADP affinity resin step. Protein preparations obtained using this purification step give unusual biphasic binding isotherms during ITC experiments (A. Gutierrez and J. Ladbury, unpublished results). This behavior was initially taken as proof of the existence of a second adenosine-binding site previously postulated from kinetics studies (*19*). However, further ITC experiments carried out with protein preparations obtained omitting the affinity step did not show this abnormal pattern. It then became apparent that the adenosine nucleotide used during elution from the 2′,5′-ADP affinity resin (i.e., 2′-AMP) remained bound to the coenzyme binding site throughout the subsequent purification steps; this artifact was at the origin of the observed multiphasic titration pattern. All the experiments reported in this work were executed with protein preparations in which the 2′,5′-ADP affinity step and/or the use of adenosine nucleotides was completely omitted. These protein preparations invariably show a coenzyme binding stoichiometry ($n$) of 1 as determined by isothermal titration calorimetry (see Discussion). Full cofactor reconstitution was achieved by incubation with freshly prepared free FAD and free FMN (5 mM) for 15 min at room temperature. The FAD and FMN content of the enzyme after reconstitution was shown to be 1:1 (cofactor:protein molar ratio) for each cofactor by reverse-phase HPLC (Waters ODS2 column) as described previously (*19*). Protein concentrations were calculated using the molar extinction coefficients previously determined: 22 000 $M^{-1}$ $cm^{-1}$ for CPR and 11 300 $M^{-1}$ $cm^{-1}$ for the FAD-binding domain (at 450 mn) (*19*).

*Isothermal Titration Calorimetry (ITC).* Protein samples for microcalorimetry experiments were prepared daily from 50% glycerol stocks kept at −20 °C. ITC experiments were conducted using a VP-ITC microcalorimeter (Microcal Inc.). Data acquisition and analysis were carried out using ORIGIN 7.0 (Microcal Inc.). Binding of ligand to CPR (or to the isolated FAD-binding domain) was quantified by fitting the evolved heat per injection to a one-set-of-sites model. Fitting of the binding isotherm was carried out through multiple iterations until a minimum $\chi^2$ value was obtained. Reported values are the average of at least two runs. ITC measurements directly determine the observed equilibrium binding constant for any given interaction, $K_{b,obs}$ ($M^{-1}$). However, in line with common usage in enzyme kinetics literature, the dissociation constant $K_d$ ($\mu$M) is preferentially used throughout the text ($K_d = 1/K_{obs}$). The concentration of the different buffering species used through out this study was 100 mM unless otherwise stated. The protein concentration used in the cell ($M_{total}$) was chosen so that $c$ values were in the 200−500 range (typically 30−15 $\mu$M). A detailed discussion of ITC data analysis has been described elsewhere (*20*, *21*). Additionally, titrations with 2′,5′-ADP were also carried out at 5 and 10 $\mu$M (protein concentration) to verify that the measured values were concentration-independent.

Temperature dependence studies for the binding equilibrium of CPR (or FAD-binding domain) with ligands (2′,5′-ADP, $NADP^+$, and $H_4NADP$) were performed over the range 5−35 °C. Two main buffers were used in these studies: potassium phosphate ($pK_2 = 7.20$) and BES ($pK_a = 7.09$). Because of the dependence of the $pK_a$ of BES on temperature ($dpK_a/dT = -0.016$), the pH of the solutions (protein and ligand) was adjusted to 7.0 at each experimental temperature. This procedure was deemed to be unnecessary when using potassium phosphate buffer ($dpK_2/dT = -0.002$). The pH dependence of 2′,5′-ADP binding was determined over a pH range of 6.0−9.5 at 25 °C. To keep the ionic strength constant, a triple-component buffer was used (ACES-Tris-ethanolamine; $I = 100$ mM) (*22*). 1,4,5,6-Tetrahydro-NADP ($H_4NADP$) was obtained by palladium-catalyzed hydrogenation of NADP(H). Two different published protocols were followed, one using NADPH (*23*) and the other using glucose-6-phosphate dehydrogenase with $NADP^+$ as the starting material (*14*). In both cases, $H_4NADP$ was purified to a final $A_{265}/A_{288}$ ratio of ≤1.3 according to protocols published elsewhere (*14*, *23*). $H_4NADP$ samples obtained by these two different methods were practically indistinguishable in terms of the ITC parameters determined from binding to CPR. However, the latter protocol using glucose-6-phosphate dehydrogenase gives considerably higher yields and rates. Formation of the 288 nm peak was complete in approximately 2 h (1 atm of 99.995% $H_2$, room temperature).

Isothermal titration calorimetry was used to study the interaction between CPR (and its isolated FMN-binding domain) and cytochrome *c*. To assess the importance of different redox states in this interaction, experiments were carried out using the one-electron reduced form. This species was induced in CPR (or FMN-binding domain) through stoichiometric titration with freshly made anaerobic dithionite stocks. Redox potentiometry (*24*) and kinetics (*11*, *19*) studies have established that this one-electron species corresponds to the high-potential blue semiquinone form of the FMN ($FMN_{ox/sq} = -66$ mV). This species accumulates easily during single-turnover reduction of the enzyme by either NADPH or dithionite, and it is remarkably resistant to air oxidation. ITC titrations with reduced species (either CPR, FMN-binding domain, or cytochrome *c*) were carried out at a low temperature (typically 10 °C).

*Pre-Steady-State Kinetic Measurements.* Association and electron transfer between CPR (or the FMN-binding domain) and cytochrome *c* were studied under single-turnover conditions using an Applied Photophysics SX.17 MV stopped-flow spectrophotometer. Unless otherwise stated, measurements with dithionite-reduced CPR (two-electron level) were carried out at 25 °C under anaerobic conditions in a glovebox (Belle Technology). All buffers were made oxygen-free by evacuation and extensive bubbling with argon before use. Cytochrome *c* reduction was monitored at 550 nm; transients were fitted using a standard single-exponential equation (*11*). Double-mixing experiments were carried out in a Biosequential SX.18MV stopped-flow spectrophotometer according to protocols provided by the manufacturer (Applied Photophysics Ltd.). An 115 $\mu$L aging loop was used for all determinations. The aging time delay between the reductive half-reaction of CPR with NADPH and binding to oxidized cytochrome *c* was varied from 20 to 10 000 ms.

## RESULTS

*Inhibitory Effect of Free Phosphate on Coenzyme Binding to CPR.* A typical binding isotherm for the interaction of oxidized CPR with $NADP^+$ in phosphate buffer is shown in Figure 2A, binding isotherm a (100 mM potassium phosphate buffer at pH 7.0 and 25 °C). The evolved heat data are

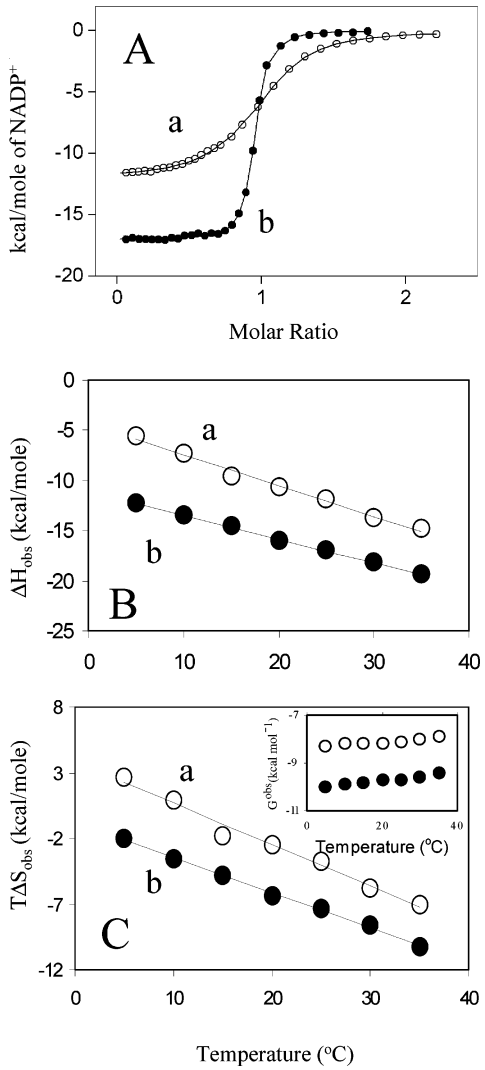


FIGURE 2: Inhibitory effect of phosphate buffer. (A) Binding isotherms for the titration of $NADP^+$ into CPR in potassium phosphate (a) and BES buffer (b) (100 mM, pH 7.0, and 25 °C). The points are fit to a one-set-of-sites model. [CPR] = 23 $\mu$M. (B) Temperature dependence of the observed enthalpy of binding ($\Delta H_{obs}$) for the CPR−$NADP^+$ interaction in potassium phosphate (plot a, ○) and BES buffer (plot b, ●) (100 mM and pH 7.0). (C) Temperature dependence of the observed entropy of binding ($T\Delta S_{obs}$) for the CPR−$NADP^+$ interaction in potassium phosphate (plot a, ○) and BES buffer (plot b, ●) (100 mM and pH 7.0). The inset of panel C shows the temperature dependence of the estimated change in Gibbs free energy ($\Delta G_{obs}$) for the CPR−$NADP^+$ interaction in potassium phosphate (○) and BES buffer (●) (100 mM and pH 7.0).

described well by a one-set-of-sites model. The calculated binding stoichiometry ($n$) is 1 (1.1 ± 0.1), indicating the binding of a single $NADP^+$ molecule to the CPR enzyme. The dissociation constant for this interaction ($K_d$) equals 760 nM. However, use of BES (100 mM, pH 7.0, and 25 °C) instead of phosphate results in a 13-fold increase in coenzyme affinity ($K_d$ = 53 nM), suggesting an inhibitory effect of phosphate buffer on binding of the coenzyme to CPR (Figure 2A, binding isotherm b) (Table 1). This higher stability of the coenzyme−CPR complex in the presence of BES is consistently observed along the temperature range that was studied, 5−35 °C (Figure 2C, inset). The temperature dependence for the enthalpy ($\Delta H_B$) and the entropy ($T\Delta S$) of binding for the $NADP^+$−CPR interaction with phosphate (plot a) and BES (plot b) is shown in panels B and C of Figure 2, respectively. The heat capacity change values ($\Delta C_p$) for the $NADP^+$−CPR interaction in the presence of phosphate and BES differ considerably: $\Delta C_p = -310$ cal $mol^{-1}$ $K^{-1}$ ($R^2$ = 0.97) and $\Delta C_p = -230$ cal $mol^{-1}$ $K^{-1}$ ($R^2$ = 0.95) for phosphate and BES, respectively (Table 2). In NADP(H)-dependent enzymes, discrimination against NAD(H) is achieved through the preferential recognition of adenosine 2′-phosphate. It is then feasible that free phosphate could interact competitively with adenosine 2′-phosphate for the phosphate binding site in the CPR enzyme. Therefore, in phosphate buffer, binding of the coenzyme to the protein would require dissociation of the prebound phosphate anion(s), replacing one interaction with another. This would be reflected in a decrease in the equilibrium binding constant for coenzyme binding (i.e., an increase in $K_d$). In housefly CPR, inorganic phosphate competitively inhibits NADPH binding with a $K_i$ of 33 mM (*14*), and binding of free phosphate to human CPR has indeed been observed during preliminary ITC experiments (A. Grunau and A. Gutierrez, unpublished results). Of particular relevance to the work presented here is the observation that free phosphate binds to cytochrome *c* at at least two distinctive sites (Lys87 and Lys25-His26-Lys27) (*25*). Binding of these phosphate molecules has a marked effect on the interaction and electron-transfer properties of cytochrome *c* with physiological and artificial redox partners (*25*). Consequently, unless otherwise stated, BES was the preferred choice over phosphate as the buffer species in the experiments reported here.

*Contribution of the Adenosine and Nicotinamide Moieties to Coenzyme Binding.* Kinetic and structural studies have firmly established the bipartite nature of NADP(H) in binding to the ferredoxin-$NADP^+$ reductase (FNR) protein family (*26*, *27*). The adenosine moiety (2′,5′-ADP) is thought to constitute the primary element in coenzyme binding. Redox chemistry exclusively involves the nicotinamide moiety [NMN(H)], which transiently interacts with the protein's redox center, an FAD molecule in CPR (Figure 1), to transfer two electrons in the form of a hydride ion. However, some controversy remains as to the nicotinamide moiety's binding mechanism and its actual contribution to binding. Recent work on cytochrome P450-$BM_3$, a protein closely related to CPR, has highlighted the possibility that the nicotinamide moiety could play a major role in coenzyme binding affinity (see Figure 6 in ref *28*). Additionally, results from molecular dynamics calculations have led to the proposal that a change in the nicotinamide ring shape that accompanies the transition from the oxidized form (NMNH, planar conformation) to the reduced form ($NMN^+$, "boat" conformation) could thus modulate binding affinity and consequently have an effect on the kinetic mechanism of hydride transfer by NAD(P)H-dependent enzymes (*16*). Data from the isothermal titration of oxidized CPR with 2′,5′-ADP are shown in Figure 3A. The observed dissociation binding constant for this interaction ($K_d$) equals 50 nM, with a binding stoichiometry $n$ of 1.0 ± 0.02 (Table 1). This $K_d$ value is practically the same as that observed for the binding of the oxidized coenzyme $NADP^+$ under the same conditions ($K_d$ = 53 nM) (Figure 2A, binding isotherm b) (Table 1). Nevertheless, the specific enthalpy (Figure 3B) and entropy (Figure 3C) contributions to $\Delta G_B$ differ significantly for each ligand. Binding of

Table 1: Thermodynamic Parameters for the Binding Interaction of CPR and the Isolated FAD-Binding Domain with Adenosine Phosphate (buffer conditions, 100 mM, pH 7.0, and 25 °C)

| ligand | buffer | temp (°C) | $n^a$ | $K_{obs}$ ($\times 10^5$ $M^{-1}$) | $K_d{}^b$ (nM) | $\Delta H_{obs}$ (kcal/mol) | $\Delta G_{obs}$ (kcal/mol) | $T\Delta S_{obs}$ (kcal/mol) |
|---|---|---|---|---|---|---|---|---|
| | | | | CPR | | | | |
| $NADP^+$ | phosphate | 25 | $1.1 \pm 0.1$ | $13 \pm 0.5$ | 760 | $-12 \pm 0.0$ | −8.3 | −3.7 |
| 2′-AMP | BES | 25 | $1.0 \pm 0.06$ | $4.7 \pm 0.6$ | 2000 | $-14 \pm 0.0$ | −7.0 | −6.9 |
| 2′,5′-ADP | BES | 25 | $1.0 \pm 0.02$ | $190 \pm 6$ | 50 | $-18 \pm 0.1$ | −9.8 | −8.2 |
| $NADP^+$ | BES | 25 | $1.1 \pm 0.01$ | $182 \pm 5$ | 53 | $-17 \pm 0.1$ | −9.6 | −7.3 |
| $H_4NADP$ | BES | 25 | $1.0 \pm 0.2$ | $142 \pm 14$ | 70 | $-19 \pm 2.0$ | −9.4 | −9.4 |
| | | | | Isolated FAD-Binding Domain | | | | |
| 2′,5′-ADP | BES | 25 | $0.9 \pm 0.2$ | $280 \pm 22$ | 37 | $-19 \pm 0.0$ | −10.3 | −9.2 |

[a] Binding stoichiometry. [b] Dissociation constant values ($K_d$) were calculated as the reciprocal of the observed equilibrium binding constant ($K_d = 1/K_{obs}$).

Table 2: Heat Capacity Changes ($\Delta C_p$) for the Binding Interaction of CPR and Isolated FAD-Binding Domain with Adenosine Phosphate Ligands (100 mM and pH 7.0)

| protein | ligand | buffer | $\Delta C_p$ (cal $mol^{-1}$ $K^{-1}$) |
|---|---|---|---|
| CPR | $NADP^+$ | phosphate | −310 |
| CPR | 2′,5′-ADP | BES | −210 |
| CPR | $NADP^+$ | BES | −230 |
| CPR | $H_4NADP$ | BES | −220 |
| FAD[a] | 2′,5′-ADP | BES | −300 |

[a] Isolated FAD-binding domain.

$NADP^+$ to CPR [Figure 3C, plot a (△)] consistently shows less unfavorable entropy changes ($T\Delta S_B$) than binding of the adenosine moiety alone (2′,5′-ADP) [Figure 3C, plot b (○)]. Fluorescence quantum yield studies have shown that, in solution, free $NADP^+$ exists primarily in an equilibrium folded conformation, with orbital stacking taking place between the adenine and the nicotinamide moieties (*29*). Binding of $NADP^+$ to protein results in the equilibrium being shifted from this folded stacked conformation to an elongated one (*29*). Crystallography studies with CPR (*30*) and ferredoxin-$NADP^+$ reductase, a FAD-binding domain analogue (*26*), show that $NADP^+$'s nicotinamide moiety does not form any interaction with the protein in the crystal complex (*30*). As indicated by the calorimetry data, this unconstrained state of the nicotinamide moiety in the coenzyme's bound form involves an entropy gain incurred in going from the stacked form to the protein complex. However, this entropy gain is accompanied by an unfavorable decrease in the enthalpy change [Figure 3B, plot a (△)]. As a consequence of this entropy−enthalpy compensation, the change in Gibbs free energy for $NADP^+$ binding ($\Delta G_B = -9.6$ kcal $mol^{-1}$) is practically the same as that for 2′,5′-ADP ($\Delta G_B = -9.8$ kcal $mol^{-1}$) (Table 1).

Heat capacity is proportional to energy fluctuations in a system and is a measure of the density of states accessible to that system (*17*). Heat capacity effects in proteins are often explained in terms of local changes in low-energy soft motional modes (vibrational, librational, and rotational modes) (*31*). In protein−small ligand interactions, the observed heat capacity changes on binding ($\Delta C_p$) have been found to correlate to burial of surface area, thus emphasizing the importance of solvation−desolvation processes (*32*−*34*). Similar $\Delta C_p$ values for binding of 2′,5′-ADP (−210 cal $mol^{-1}$ $K^{-1}$, $R^2 = 0.99$) and $NADP^+$ (−230 cal $mol^{-1}$ $K^{-1}$, $R^2 = 0.93$) (Table 2) indicate that no significant change in the binding surface originates from the additional presence of the $NMN^+$ moiety.

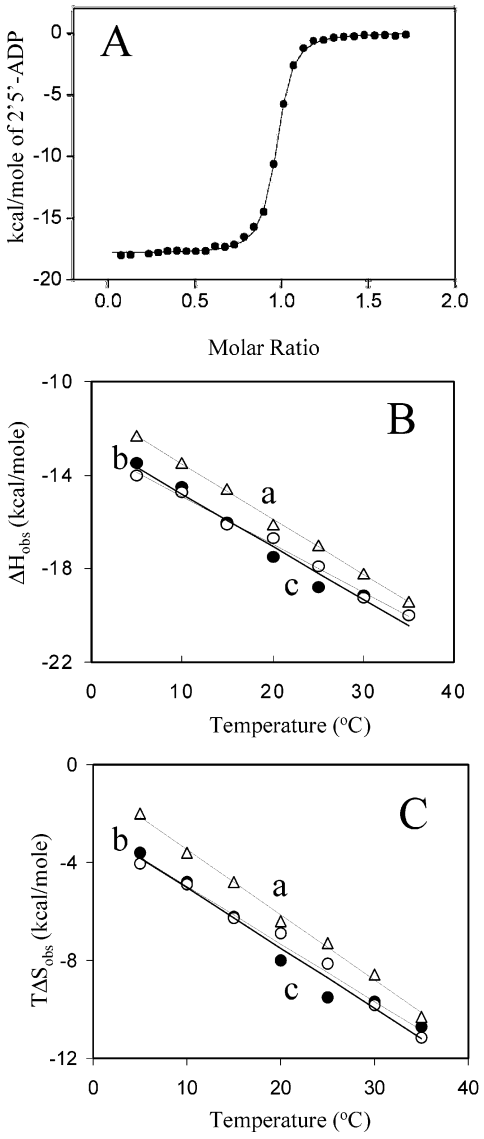


FIGURE 3: Isothermal titration of oxidized CPR with 2′,5′-ADP, $NADP^+$, and $H_4NADP$. BES buffer (100 mM, pH 7.0, and 25 °C). (A) Binding isotherms for the titration of 2′,5′-ADP into CPR (17−25 μM). The points are fit to a one-set-of-sites model. (B) Temperature dependence of the observed enthalpy of binding ($\Delta H_{obs}$) to CPR for $NADP^+$ (plot a, △), 2′,5′-ADP (plot b, ○), and $H_4NADP$ (plot c, ●). (C) Temperature dependence of the observed entropy of binding ($T\Delta S_{obs}$) to CPR for $NADP^+$ (plot a, △), 2′,5′-ADP (plot b, ○), and $H_4NADP$ (plot c, ●).

Isothermal titration calorimetry was used to study the binding of 1,4,5,6-tetrahydro-NADP ($H_4NADP$), an isosteric NADPH analogue. $H_4NADP$ is inert as an electron source.

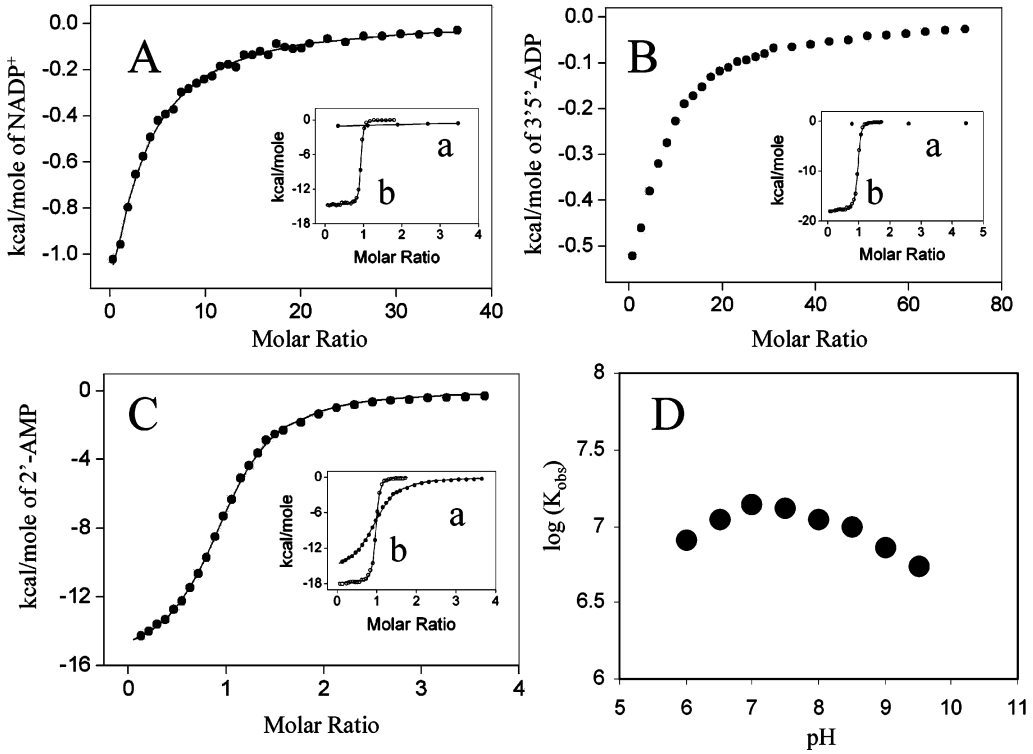


FIGURE 4: Calorimetric titration experiments with the R597A CPR mutant, 3′,5′-ADP, and 2′-AMP. (A) Binding isotherm for the titration of $NADP^+$ into the R597A CPR mutant (25 $\mu$M). In the inset, binding isotherms for binding of $NADP^+$ to the R597A mutant (a) and wild-type CPR (b) are shown together for comparative purposes. Notice the dramatic decrease in molar enthalpy due to the loss of the 2′-phosphate interaction upon removal of R597. BES buffer (100 mM, pH 7.0, and 25 °C). (B) Binding isotherm for the titration of 3′,5′-ADP into wild-type CPR (25 $\mu$M). In the inset, binding isotherms for binding of 3′,5′-ADP (a) and 2′,5′-ADP (b) to wild-type CPR are shown together for comparative purposes. BES buffer (100 mM, pH 7.0, and 25 °C). (C) Binding isotherm for the titration of 2′-AMP into wild-type CPR (20 $\mu$M). In the inset, binding isotherms for binding of 2′-AMP (a) and 2′,5′-ADP (b) to wild-type CPR are shown together for comparative proposes. BES buffer (100 mM, pH 7.0, and 25 °C) (D) pH dependence of the equilibrium binding constant ($K_{b,obs}$) for binding of 2′,5′-ADP to wild-type CPR. To keep the ionic strength constant ($I$ = 100 mM), a triple-component buffer was used (ACES-Tris-ethanolamine).

However, like NADPH, it carries one extra hydrogen at the pyridinium ring's C4 atom (the opposite of that of $NADP^+$). This is likely to lie behind the observation that $H_4NADP$'s pyridinium ring has a three-dimensional structure resembling that of NADPH (the so-called "flat" conformation) (*14*). Competitive inhibition studies with housefly CPR indicate that $H_4NADP$ does indeed behave as a good NADPH analogue (*14*). Use of $H_4NADP$ thus allows an accurate reproduction of the interaction between the reduced nicotinamide and the oxidized FAD isoalloxazine ring without hydride transfer taking place. The dissociation constant for the binding of $H_4NADP$ to CPR ($K_d$ = 70 nM) is basically the same as that for 2′,5′-ADP ($K_d$ = 50 nM) and $NADP^+$ ($K_d$ = 53 nM) (Table 1). The similarity between the binding energetics of $H_4NADP$ and those of the 2′,5′-ADP moiety is also evident when the data for the temperature dependence of the enthalpy ($\Delta H_B$) and entropy ($T\Delta S_B$) of binding for these ligands are compared (panels B and C of Figure 3, respectively), as the two plots superimpose [2′,5′-ADP, plot b (○); $H_4NADP$, plot c (●)]. The change in heat capacity ($\Delta C_p$) for $H_4NADP$ (−220 cal $mol^{-1}$ $K^{-1}$, $R^2$ = 0.96) is identical to that of 2′,5′-ADP (−210 cal $mol^{-1}$ $K^{-1}$, $R^2$ = 0.99) and that of $NADP^+$ (−230 cal $mol^{-1}$ $K^{-1}$, $R^2$ = 0.93) (Table 2).

Results from ITC experiments with 2′,5′-ADP, $NADP^+$, and $H_4NADP$ point toward the preeminence of the adenosine over the nicotinamide moiety in determining the energetics of coenzyme binding in CPR. The recognition and stability of the coenzyme−CPR complex are thus largely determined by interaction with adenosine 2′-phosphate. This conclusion is corroborated by binding studies carried out with the R597A CPR mutant (Figure 4A). In the crystal structure of the CPR−$NADP^+$ complex (*30*), the adenosine 2′-phosphate binding pocket is formed by R298, S596, R597, K602, and Y604; the R597 residue is positioned to form a salt bridge interaction with the 2-phosphate (Figure 1). As shown in Figure 4A, destruction of this interaction in the R597A mutant leads to severe impairment of binding of $NADP^+$ to CPR, the molar enthalpy of binding ($\Delta H_B$) being reduced from −17 kcal $mol^{-1}$ (wild type) to −1 kcal $mol^{-1}$ (R597A). The dissociation constant ($K_d$) for 2′,5′-ADP binding by the R597A mutant is 160 $\mu$M. This amounts to an ∼3000-fold decrease in the stability of the coenzyme−CPR complex, brought about by removal of R597 (Figure 4A, inset). Remarkably, recognition of the phosphate group at position 2′ is highly precise, since 3′,5′-ADP binds very weakly to wild-type CPR (Figure 4B and its inset). Although interaction between adenosine 2′-phosphate and R597 is the indisputable primary source for binding energy and coenzyme discrimination, differences between 2′,5′-ADP ($K_d$ = 50 nM, $\Delta G_B$ = −9.8 kcal $mol^{-1}$) and 2′-AMP ($K_d$ = 2 $\mu$M, $\Delta G_B$ = −7 kcal $mol^{-1}$) (Figure 4C) indicate a synergy involving secondary interactions between the 5′-phosphate group and another basic residue from the binding site (different from R597). Indeed, 5′,5′-ADP binds to CPR, albeit significantly weaker than 2′,5′-ADP ($K_d$ = 78 $\mu$M, $\Delta G_B$ = −5.5 kcal $mol^{-1}$, figure

not shown). On the basis of the crystal structure of the NADP$^+$−CPR complex, R298 would be the most likely residue to interact with the 5′-phosphate group (Figure 1B).

Earlier, Sem and Kasper used steady-state kinetics to identify ionizable groups involved in binding of the coenzyme to CPR (*35*). They concluded that the 2′-phosphate group of NADP$^+$ binds as the dianion and that arginine 597 must be protonated for optimum binding with p$K_a$ values for 2′-phosphate (in NADP$^+$) and Arg597 of 5.95 and 9.53, respectively (*35*). A plot of the pH dependence of $K_{b,obs}$ for the binding of 2′,5′-ADP to CPR is shown in Figure 4D. The data describe a typical arch denoting the existence of at least two ionizable groups. This is qualitatively consistent with the conclusions found in kinetics studies described above, and once again it highlights the critical role of the interaction between 2′-phosphate and R597.

*Global Effects on the Energetics of Binding of the Coenzyme to CPR.* Recent temperature-jump studies with the CPR enzyme indicate that interdomain electron transfer is strongly gated by diffusional motion required to bring the FAD and FMN-binding domains into a favorable orientation (*11*). Further relaxation kinetics studies showed that binding of 2′,5′-ADP or 2′-AMP leads to a 3-fold increase in interdomain electron-transfer rates (*12*), suggesting that the binding of these ligands can bring the two domains into a kinetically productive conformation (*12*). Early fluorescence energy-transfer (FRET) studies with ligand-free CPR concluded that in solution the two flavins could be separated by as much as 20 Å (*36*), while in the crystal structure of the NADP$^+$−CPR complex, this inter-flavin distance is found to be only 4 Å (*30*). These observations indicate a broad scope of domain movements taking place in this protein. By comparing the thermodynamic parameters of binding of 2′,5′-ADP to the isolated FAD-binding domain to those obtained with intact CPR, we aimed to identify any linkage between coenzyme binding energetics and domain−domain conformational rearrangements.

Previous single-turnover kinetics studies with the two isolated domains showed that although they are kinetically competent, they do not form a stable complex (*19*). NMR titration studies of the $^{15}$N-labeled FMN-binding domain with the FAD-binding domain failed to observe any chemical shift changes indicative of complex formation (*19*). Indeed, no significant interaction between the isolated domains could be detected by ITC (A. Grunau and A. Gutierrez, unpublished results). This absence of strong interaction between the two domains also seems to be characteristic of intact CPR, as indicated by the fact that midpoint redox potentials of the two isolated domains are identical to those in the intact CPR molecule (*24*). The dissociation constant ($K_d$) for binding of 2′,5′-ADP to the FAD-binding domain at 20 °C is 37 nM (Table 1). This value is close to that obtained for the binding of 2′,5′-ADP to CPR ($K_d$ = 50 nM). This similarity in 2′,5′-ADP dissociation constant values for CPR and the isolated FAD-binding domain is not unexpected and reflects the fact that the coenzyme binding site is fully contained within the FAD-binding domain (Figure 1) (*30*). Nevertheless, the specific energetics of the two binding events are noticeably different (Figure 5). A plot for the temperature dependence of $\Delta H_B$ for binding of 2′,5′-ADP to the isolated FAD-binding domain [Figure 5A, plot b (○)] systematically diverges downward from that observed with CPR [Figure 5A, plot a (●)] as the temperature increases. As a consequence, their associated heat capacity changes are markedly different: $\Delta C_p$ = −210 cal mol$^{-1}$ K$^{-1}$ ($R^2$ = 0.99) and −300 cal mol$^{-1}$ K$^{-1}$ ($R^2$ = 0.95) for CPR and the isolated FAD-binding domain, respectively (Table 2). The magnitude of this difference (a 50% increase) is significant and compares well with $\Delta\Delta C_p$ values observed with single-point mutations of residues found to be important in the heat capacity effect of biological interactions (*37*). Therefore, binding of the coenzyme to the FAD-binding domain impinges on events involving the FMN-binding domain. This is remarkable since the 2′,5′-ADP binding pocket is located in a solvent-exposed cleft, with no shared surface between this binding motif and the FMN-binding domain (Figure 1). A similar pattern is unveiled by examining entropy changes ($T\Delta S_B$) across a similar temperature range (5−35 °C; Figure 5B and Table 1). The entropy change values ($T\Delta S_B$) for binding of 2′,5′-ADP to CPR (i.e., in the presence of the FMN-binding domain) are consistently higher (i.e., more favorable) than those for binding of the same ligand to the isolated FAD-binding domain (Figure 5B, plots a and b, respectively). At 35 °C, this difference amounts to 2 kcal mol$^{-1}$: $T\Delta S_B$ = −13 and −11 kcal mol$^{-1}$ for the isolated FAD-binding domain and CPR, respectively. This entropy gain amounts to a contribution of roughly 2 orders of magnitude to the observed equilibrium binding constant $K_{b,obs}$. Thus, the number of accessible conformational substates of the protein increases with 2′,5′-ADP binding in the presence of the FMN-binding domain. These results point toward a global

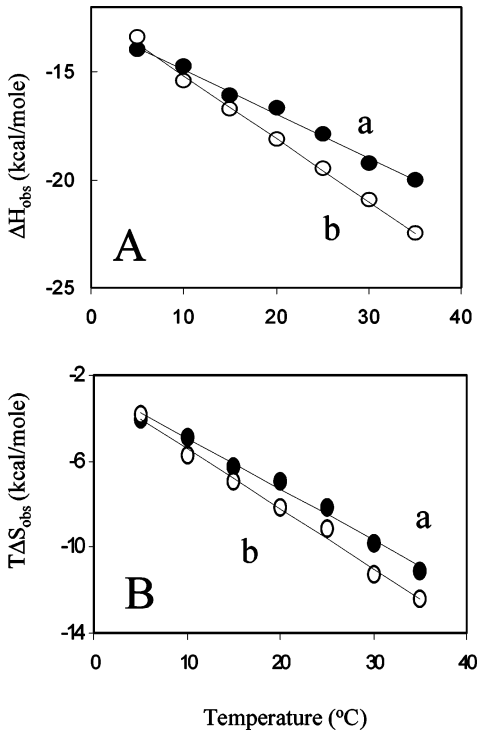


FIGURE 5: Thermodynamics of binding of 2′,5′-ADP to the isolated FAD-binding domain. BES buffer (100 mM, pH 7.0). The FAD-binding domain concentration was 17−22 $\mu$M. Lines represent the linear least-squares regression to the experimental data. Each point is the average of at least three independent measurements. (A) Temperature dependence of the observed enthalpy of binding ($\Delta H_{obs}$) for intact CPR (plot a, ●) and the isolated FAD-binding domain (plot b, ○). (B) Temperature dependence of the observed entropy of binding ($T\Delta S_{obs}$) for intact CPR (plot a, ●) and the isolated FAD-binding domain (plot b, ○).

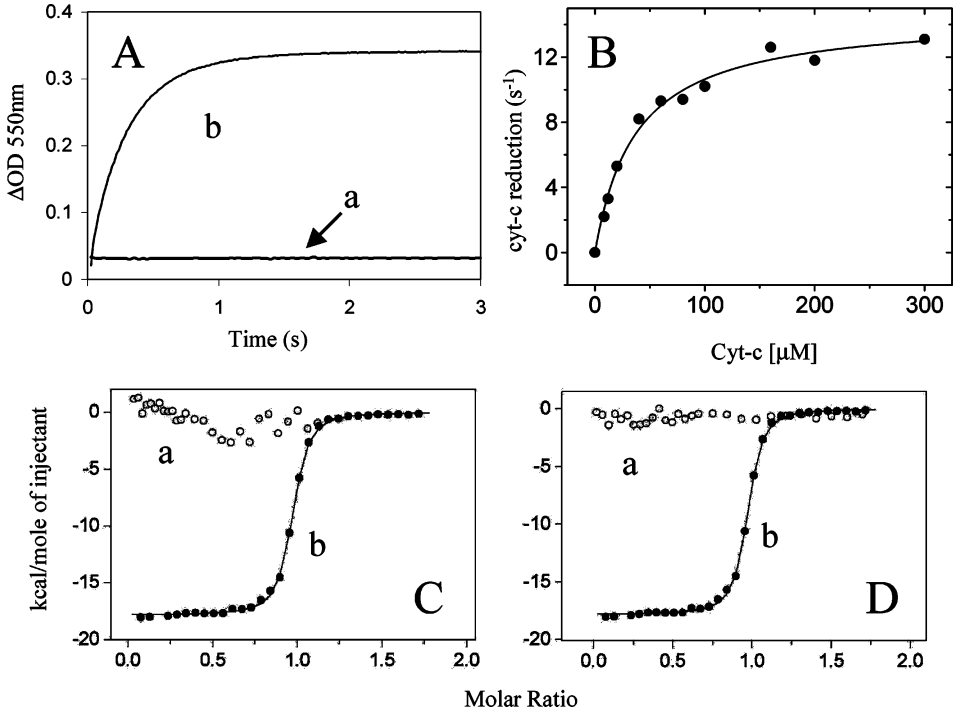


FIGURE 6: CPR−cytochrome *c* interaction. (A) Transient a is that obtained from rapid mixing experiments with prereduced CPR and oxidized cytochrome *c*. CPR (10 $\mu$M) was reduced to the one-electron level (FMN semiquinone species, $FMN_{sq}$) by stoichiometric titration with dithionite under anaerobic conditions. The CPR sample was allowed to equilibrate (5−10 min) prior to mixing with cytochrome *c* at the saturation concentration (200 $\mu$M). Transient b is that obtained for cytochrome *c* reduction from rapid mixing experiments in which oxidized CPR (10 $\mu$M) (syringe A) was mixed against a mixture of equimolar NADPH (10 $\mu$M) and oxidized cytochrome *c* (200 $\mu$M) (syringe B). Data are best described by a single-exponential expression, yielding a value for $k_{obs}$ of 12 $s^{-1}$. Conditions: 100 mM BES buffer, pH 7.0, and 25 °C. (B) Dependence of the observed rates of cytochrome *c* reduction by CPR (10 $\mu$M). Mixing conditions as for transient b in panel A. Apparent $k_{max} = 14$ $s^{-1}$, and apparent $K_d = 37$ $\mu$M. Conditions: 10 $\mu$M NADPH, 100 mM BES buffer, pH 7.0, and 25 °C. (C) Titration of oxidized CPR (25 $\mu$M) with oxidized cytochrome *c* (600 $\mu$M) (binding isotherm a, ○). Titration of 2′,5′-ADP into CPR (17−25 $\mu$M) is shown for comparative purposes (binding isotherm b, ●), with conditions as described in the legend of Figure 3A. (D) Titration of one-electron prereduced CPR (25 $\mu$M) with oxidized cytochrome *c* (600 $\mu$M) (binding isotherm a, ○) and CPR reduction by dithionite as described for panel A. Titration of 2′,5′-ADP into CPR (17−25 $\mu$M) is shown for comparative purposes (binding isotherm b, ●), with conditions as described in the legend of Figure 3A.

effect of coenzyme binding in the energetics of the entire CPR molecule.

*Calorimetry and Kinetics Studies of the Interaction of CPR and Its Isolated FMN-Binding Domain with Cytochrome c.* Cytochrome *c*, a key mitocondrial electron-transfer protein, has long been known to be a good redox partner for the CPR enzyme, cytochrome *c* reduction becoming the standard assay for steady-state kinetics studies of CPR (*1*). Electron transfer to cytochrome *c* proceeds via the FMN-binding domain (*16*). Cytochrome *c* can also accept electrons from the reductase domains of P450-$BM_3$ and NOS, two proteins from the CPR family, in essentially the same manner, from FMN to heme (*16*).

A kinetic transient from stopped-flow spectroscopy measurements of cytochrome *c* reduction by CPR under a pseudostoichiometric amount of NADPH is shown in Figure 6A (transient b). Likewise, under steady-state conditions (*1*, *38*), single-turnover reduction of cytochrome *c* by CPR shows saturation kinetics with a $k_{max}$ of 14 $s^{-1}$ and an apparent $K_d$ of 37 $\mu$M (Figure 6B). We have previously shown that under pseudostoichiometric NADPH conditions, hydride transfer from NADPH and formation of the blue disemiquinoid species ($FAD_{sq}/FMN_{sq}$) occur very fast, reaching completion within the first 50 ms (70 $s^{-1}$) (*11*, *19*). However, electron transfer from FMN to cytochrome *c* occurs 4 times slower ($k_{max} = 14$ $s^{-1}$; Figure 6B). This low rate constant for electron transfer from FMN to cytochrome *c* is likely to reflect rate-limiting steps involved in the formation of a productive bimolecular complex (a second-order process) and subsequent energy level equalization (activation) that must take place prior to the actual isoenergetic electron-transfer step (*39*).

Cytochrome *c* has an asymmetric charge distribution that results in a molecular dipole moment of ∼300 D (*40*). This dipole is thought to orient cytochrome *c* such that the heme edge at the positive end faces the redox partner, thus contributing to the formation of a kinetically productive complex. Crystallography (*41*) and NMR (*42*) studies of CPR and the FMN-binding domain show that this domain is also strongly dipolar, with a dipole moment ∼680 D (*41*). A model for the CPR−cytochrome *c* complex was proposed on the basis of maximizing the contacts between the positively charged cytochrome *c* surface and the mostly negatively charged FMN surface, implicating a leading role for dipole complementarity in this interaction (*30*). In this model, cytochrome *c* lies in a "bowl", the interacting surface largely provided by $\beta$4−$\alpha$6 (residues 175−182) and $\beta$5−$\alpha$7 (residues 207−211) loops from the FMN-binding domain (see Figure 5 of ref *30*). In sharp contrast to what was predicted from this protein complex model, no enthalpy changes were observed during titration of CPR with cytochrome *c* (Figure 6C, binding isotherm a). A similar pattern was observed at 5, 15, and 30 °C (data not shown).

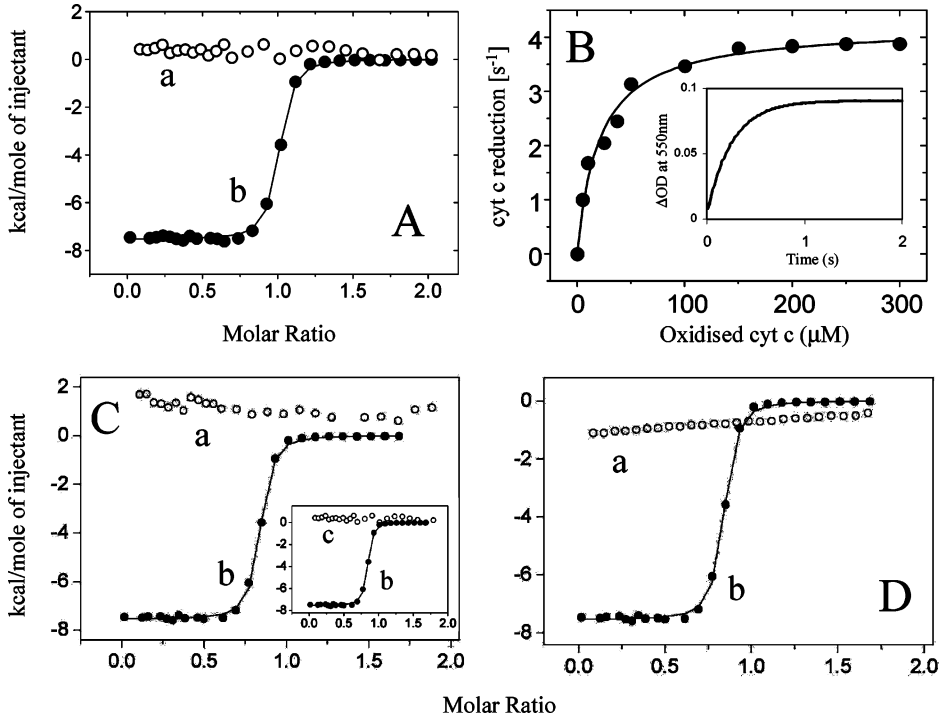


FIGURE 7: Binding and electron transfer between the isolated FMN-binding domain and cytochrome *c*. *(A) Titration of oxidized (binding isotherm a, ○) and one-electron reduced (dithionite reduction) (binding isotherm b, ●) FMN-binding domain (25 $\mu$M) with oxidized cytochrome *c* (600 $\mu$M). Conditions: 100 mM BES buffer, pH 7.0, and 25 °C. (B) Dependence of the observed rates of cytochrome *c* reduction by the isolated FMN-binding domain (10 $\mu$M). Apparent $k_{max} = 4.2\ s^{-1}$, and apparent $K_d = 21\ \mu$M. Conditions: 10 $\mu$M NADPH, 100 mM BES buffer, pH 7.0, and 25 °C. In the inset is the transient obtained for cytochrome *c* reduction from rapid mixing experiments in which the oxidized FMN-binding domain (10 $\mu$M) (syringe A) was mixed against a mixture of equimolar NADPH (10 $\mu$M) and oxidized cytochrome *c* (200 $\mu$M) (syringe B). (C) Titration of the oxidized FMN-binding domain (20 $\mu$M) with one-electron reduced cytochrome *c* (600 $\mu$M) (dithionite reduction) (binding isotherm a, ○). Binding isotherm b (●) is the same as binding isotherm b in panel A. In the inset, binding isotherm c (○) is titration of one-electron reduced FMN-binding domain (20 $\mu$M) against one-electron reduced cytochrome *c* (600 $\mu$M) (dithionite reduction). (D) Titration of the oxidized FMN-binding domain (20 $\mu$M) with bovine serum albumin (600 $\mu$M) (binding isotherm a, ○). Binding isotherm b (●) is the same as binding isotherm b in panel A.

One-electron reduction of CPR by dithionite results in the formation of an air-stable blue semiquinone in the FMN ($FMN_{ox/sq} = -66$ mV) (see Experimental Procedures). Single-turnover rapid-mixing experiments of one-electron reduced CPR (dithionite) with oxidized cytochrome *c* failed to detect reduction of cytochrome *c* ($Fe^{3+} \rightarrow Fe^{2+}$, $\lambda = 550$ nm) (Figure 6A, transient a). Similarly, ITC experiments failed to detect any interaction between one-electron reduced CPR and oxidized cytochrome *c* (Figure 6D, binding isotherm a). This situation resembles that observed with the oxidized CPR and the oxidized cytochrome *c* (Figure 6C, binding isotherm a). This absence of enthalpy changes indicates that the failure to observe electron transfer between dithionite-reduced CPR and oxidized cytochrome *c* by stopped-flow methods (Figure 6A, transient a) is indeed due to the absence of any interaction between the two proteins. This inability of dithionite-reduced CPR to reduce cytochrome *c* resembles inhibition of housefly CPR following reduction and incubation of this enzyme (10 min) with NADPH (*43*).

A valuable insight into the reasons for the absence of interaction between cytochrome *c* and CPR (either oxidized or dithionite-reduced form) is provided by calorimetry titrations using the isolated FMN-binding domain (Figure 7). Like oxidized CPR, the oxidized isolated FMN-binding domain does not interact with oxidized cytochrome *c* (Figure 7A, binding isotherm a). Remarkably, it is only when the one-electron reduced FMN semiquinone, $FMN_{sq}$ (induced by dithionite titration), is employed that interaction with oxidized cytochrome *c* can be observed (Figure 7A, binding isotherm b). This interaction is nicely described by a saturation binding isotherm which shows the expected binding stoichiometry (*n*) value of 1 ($1.1 \pm 0.2$) (Figure 7A, binding isotherm b). The dissociation constant ($K_d$) for this interaction is 47 nM (Figure 7A). This interaction between the reduced FMN-binding domain and the oxidized cytochrome *c* observed during ITC experiments does result in efficient electron transfer (i.e., cytochrome *c* reduction) as determined by rapid-mixing stopped-flow experiments (Figure 7B). Cytochrome *c* reduction by the semiquinone FMN ($FMN_{sq}$) obeys a Michaelis mechanism involving a fast binding equilibrium step followed by irreversible electron transfer with an apparent $k_{max}$ of 4.2 $s^{-1}$ and an apparent $K_d$ of 21 $\mu$M (Figure 7B). This kinetic evidence for a true binding equilibrium between the one-electron reduced FMN-binding domain and oxidized cytochrome *c* lends support to our interpretation of the isothermal calorimetry data for this interaction (Figure 7A, binding isotherm b). Therefore, in the isolated FMN-binding domain, formation of a kinetically competent complex is critically dependent on the presence of a one-electron species (i.e., semiquinone FMN, $FMN_{sq}$). This observation points toward local differences, conformational and/or electrostatic, between the oxidized and reduced FMN-binding domain. Further work will be required to understand the mechanism behind these changes as well as the apparent adiabatic nature of

the actual electron-transfer step between these two proteins (*39*).

The one-electron reduced cytochrome *c* (dithionite) does not show any binding affinity for either the oxidized FMN-binding domain (Figure 7C, binding isotherm a) or the one-electron reduced FMN-binding domain (Figure 7C, inset). Fundamental considerations about steady-state kinetics would indeed postulate that the affinity of the FMN-binding domain for cytochrome *c* should decrease once electron transfer takes place to facilitate the binding of a new oxidized cytochrome *c* molecule. The molecular recognition behind this interaction seems to be highly specific as judged by results shown in Figure 7D. ITC experiments in which the one-electron dithionite-reduced FMN-binding domain was titrated against another globular protein (bovine serum albumin) failed to detect any significant interaction (Figure 7D, binding isotherm a).

These results obtained using the one-electron reduced FMN-binding domain ($FMN_{sq}$) (Figure 7) contrast with the failure to observe either binding interaction or electron transfer to cytochrome *c* when the same redox form ($FMN_{sq}$) is induced in the CPR enzyme (Figure 6A,C,D). This leads the conclusion that, in the full CPR enzyme, the FMN-binding domain must be secluded from interacting with cytochrome *c*. This observation is reminiscent of the redox-inert locked semiquinone species previously observed in housefly CPR (*43*). Kinetics and EPR spectroscopy studies in this enzyme show the emergence of a catalytically noncompetent FMN semiquinone ($FMN_{sq}$) after incubation for 10 min with NADP(H). This "air-stable" inactive FMN semiquinone ($FMN_{sq}$) is thought to be kinetically stabilized upon conformational drifting into a "locked" form (*43*).

The lack of interaction between oxidized CPR and oxidized cytochrome *c* is really surprising, especially in light of previous electrostatics (*41*) and docking studies (*30*). Calorimetry studies have shown that the oxidized cytochrome *c* does bind to the oxidized cytochrome *c* oxidase (*44*). Therefore, this is not a general feature of interactions of cytochrome *c* with other redox proteins, but rather, it appears to derive from the intrinsic properties of CPR's domains. Early work on the formation of a covalent complex between rat CPR and horse cytochrome *c* concluded that for chemical cross-linking to take place, CPR had to be reduced by NADPH, suggesting a lack of interaction between the fully oxidized species (*45*, *46*). Previous redox potentiometry (*24*) and temperature-jump (*11*) studies with CPR have demonstrated that reduction to the two-electron level leads to an equilibrium mixture of FMN semiquinone ($FMN_{ox/sq} = -66$ mV), FMN hydroquinone ($FMN_{sq/hq} = -269$ mV), and FAD semiquinone ($FAD_{ox/sq} = -283$ mV) species. No electron transfer between CPR and cytochrome *c* was detected even upon induction of both donor species ($FMN_{sq}$ and $FMN_{hq}$) by dithionite reduction (Figure 8A, transient a). The presence of these dithionite-induced species equally failed to drive any binding interaction with oxidized cytochrome *c* during ITC experiments (data not shown). This indicates that the presence of electrons in the FMN cofactor is not by itself capable of driving the formation of a kinetically productive complex between CPR and cytochrome *c*. Accordingly, in the intact CPR, a purely redox-dependent mechanism does not appear to be behind the conformational rearrangements leading to the FMN-binding domain being exposed to cytochrome *c*. Indeed, NMR studies with the dithionite-reduced FMN-binding domain (hydroquinone form, $FMNH_2$) failed to reveal any major redox-dependent conformational changes in the isolated FMN-binding domain (*42*).

Electron transfer between the full CPR and cytochrome *c* does take place when the physiological coenzyme NADPH is used as the electron source (Figure 6A, transient b, and Figure 6B). It then becomes apparent that coenzyme−protein interaction is the key element in the FMN-binding domain overcoming its constrained state. This ultimately results in an efficient interaction with cytochrome *c* and concomitant electron transfer. Further experimental evidence of this is provided by sequential rapid-mixing experiments described in Figure 8B−D. In these experiments, CPR is reacted with a stoichiometric amount of NADPH and then different aging times (from 20 to 10 000 ms) are set prior to bringing CPR into contact with oxidized cytochrome *c* at a saturating concentration (200 $\mu$M). Aging times thus report on the time elapsed from the onset of any conformational dynamics in CPR triggered by coenzyme binding. As shown in Figure 8B, the extent of cytochrome *c* reduction (judged by the amplitude changes at $\lambda = 550$ nm, $Fe^{3+} \rightarrow Fe^{2+}$) rapidly decreases with an increase in aging times; a time delay of just 20 ms leads to an approximately 25% decrease (Figure 8B, transient b). This sharp dependence of the extent of cytochrome *c* reduction on CPR's aging times follows an exponential decay pattern, with a half-time $\tau_{50}$ of $330 \pm 70$ ms (Figure 8C). The rates of cytochrome *c* reduction also show a similar pattern, with a half-time $\tau_{50}$ of $1200 \pm 550$ ms (Figure 8D). In view of the evidence presented in Figures 6 and 7, this fast loss of CPR's ability to form a kinetically productive complex with cytochrome *c* might reflect its conversion to a conformer with a structurally locked FMN-binding domain (*43*). It then becomes evident that the harnessing of coenzyme binding energy in the formation of a kinetically productive CPR−cytochrome *c* complex is a highly synchronized event.

## DISCUSSION

We had previously proposed the existence of a second adenosine phosphate binding site in CPR based on pre-steady-state kinetic studies (*19*). It was then suggested that a decrease in hydride-transfer rates at high NADPH concentrations was due to the steric hindrance caused by two coenzyme molecules binding simultaneously. A similar decrease in hydride-transfer rates at high NADPH concentrations was subsequently observed in nitric oxide synthase, NOS (*48*), and P450-$BM_3$ (*28*), members of the CPR-diflavin reductase family, and in FprA, an adrenodoxin reductase homologue (*49*). However, the proposal of a second coenzyme binding site is highly controversial since all the reported crystal structures of CPR (*30*, *50*), and those of related proteins such as NOS (*51*), show only one bound $NADP^+$ molecule. An alternative single-binding-site kinetic model has recently been proposed by Daff (*52*). According to this model, the observed negative dependence of flavin reduction rates would originate from the reversible nature of the hydride-transfer step between NADP(H) and FAD-($H_2$) (*19*, *52*). This model satisfactorily explains the data for wild-type P450-$BM_3$ and mutants in which the putative second binding site had been deleted (*28*). The calorimetry data presented here contribute decisively to resolution of the

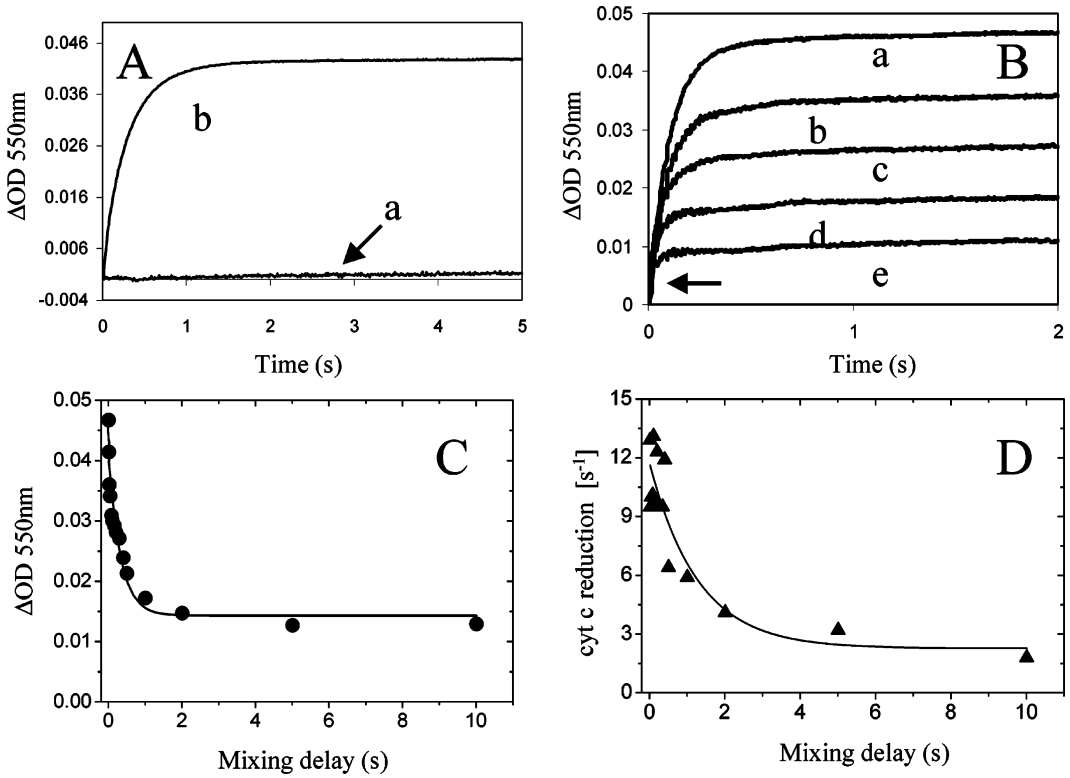


FIGURE 8: Sequential mixing stopped-flow studies of cytochrome *c* reduction by CPR. (A) Transient a is that obtained from rapid mixing experiments with two-electron prereduced CPR and oxidized cytochrome *c*. CPR (10 $\mu$M) was reduced to the two-electron level by stoichiometric titration with dithionite under anaerobic conditions. Introduction of two electron equivalents in the CPR enzyme leads to the formation of both redox species in the FMN (i.e., semiquinone and hydroquinone). Transient b is that obtained for cytochrome *c* reduction from single mixing experiments in which oxidized CPR (10 $\mu$M) (syringe A) was mixed against a mixture of equimolar NADPH (10 $\mu$M) and oxidized cytochrome *c* (200 $\mu$M) (syringe B). Data are best described by a single-exponential expression, yielding a value for $k_{obs}$ of 12 $s^{-1}$. Conditions: 100 mM BES buffer, pH 7.0, and 25 °C. (B) Kinetic transients for cytochrome *c* reduction obtained from sequential mixing experiments. The first mixing event is NADPH (20 $\mu$M) vs CPR (20 $\mu$M). The second mixing event is cytochrome *c* (200 $\mu$M). Only a selection of transients are shown for clarity. Mixing delay times (milliseconds): 0 (a), 20 (b), 29 (c), 1000 (d), and 10 000 (e). An arrow indicates an initial burst phase reporting on charge-transfer species between NADP(H) and FAD (*11*, *38*). (C) Dependence of the extent of cytochrome *c* reduction ($\Delta$OD = 550 nm) on mixing delay times. The curve represents fitting of the data to a first-order exponential decay equation (Origin 7.0). Estimated half-time $\tau_{50} = 330 \pm 70$ ms. (D) Dependence of cytochrome *c* reduction on mixing delay times. The curve represents fitting of the data to a first-order exponential decay equation (Origin 7.0). Estimated half-time $\tau_{50} = 1200 \pm 500$ ms.

controversy surrounding these conflicting kinetic models. No evidence for a second binding site (i.e., binding stoichiometry $n = 2$) was observed during isothermal titration calorimetry experiments performed with 2′,5′-ADP, $NADP^+$, or $H_4$-NADP. Initial ITC data showing biphasic binding isotherms (i.e., $n = 2$) were found to be an artifact originating from 2′-AMP contamination during CPR purification (see Experimental Procedures). There is therefore no physical basis for our two-binding-sites model (*19*). The one-site model proposed by Daff (*52*) thus aptly explains the negative NADPH dependence of hydride-transfer rates observed during the reductive half-reaction of human CPR.

The results presented here indicate the preeminence of the adenosine 2-phosphate moiety over the nicotinamide moiety in determining the stability of the coenzyme−CPR complex (expressed as $\Delta G_B$). The dissociation binding constants for $NADP^+$ ($K_d = 80$ nM) and $H_4$NADP ($K_d = 100$ nM) are strikingly similar to that for 2′,5′-ADP ($K_d = 76$ nM). Therefore, the redox state of the nicotinamide moiety appears to have no effect whatsoever on the coenzyme's affinity for the oxidized CPR enzyme. Predictably, some differences do arise in the entropy contribution of the nicotinamide moiety (Figure 3C). However, its net contribution to $\Delta G_B$, and therefore to the dissociation binding constant, is practically nil due to entropy−enthalpy compensation phenomena (Figure 3B and Table 1). Equally, the observation of similar heat capacity change ($\Delta C_p$) values for the binding of 2′,5′-ADP (−210 cal $mol^{-1}$ $K^{-1}$), $NADP^+$ (−230 cal $mol^{-1}$ $K^{-1}$), and $H_4$NADP (−220 cal $mol^{-1}$ $K^{-1}$) (Table 2) indicates no significant contribution from the nicotinamide moiety to the binding interaction surface. Although interaction between adenosine 2′-phosphate and R597 is the indisputable primary source for binding energy and coenzyme discrimination, the difference between 2′-AMP ($\Delta G_B = -7$ kcal $mol^{-1}$) and 2′,5′-ADP ($\Delta G_B = -9.8$ kcal $mol^{-1}$) indicates a synergy involving secondary interactions between R298 and the coenzyme's 5′-phosphate (Figure 1B). These results suggest that the intrinsic on and off rates for the adenosine 2′-phosphate−R597 interaction (equilibrium thermodynamics) are some of the main determinants of the observed rates of coenzyme exchange during catalytic turnover. However, the contribution of nonequilibrium interactions to coenzyme exchange rates should also be considered. Redox-dependent charge-transfer complex(es) between the nicotinamide moiety and FAD's isoalloxazine ring, and the concomitant displacement of an aromatic residue (Trp676 in human CPR), are likely to contribute to the observed steady-state coenzyme exchange rates (*27*, *38*, *47*).

Protein electron-transfer reactions are kinetically gated by the diffusional motion required to sample configurations with

favorable tunneling distances (*53*−*55*). Therefore, conformational dynamics affecting the relative position of redox cofactor-binding domains are likely to be a general feature of biological redox processes. Early mutagenesis studies on the interaction of CPR with cytochrome P450 2D6 and cytochrome *c* suggested that to shuttle electrons from the FAD to the heme protein partner, the FMN-binding domain would have to "swing" in and out in relation to the rest of the CPR molecule (*41*, *56*). The FMN-binding domain would then form mutually exclusive complexes with its electron-donating and electron-accepting partners. NMR studies on the methionine synthase system, a homologue to the CPR−cytochrome P450 complex, lend further support to this model (*57*).

A remarkable finding in these studies is that binding of the coenzyme to the FAD-binding domain has an effect on the binding energetics and protein-interaction properties of the entire CPR molecule. In the CPR molecule, the spatial arrangement of the coenzyme and cofactors binding sites reflects the physiological direction of electron flow: NADPH → FAD → FMN → heme (P450). There is no shared surface between this binding pocket and the FMN-binding domain (Figure 1) (*30*). Nevertheless, binding of 2′,5′-ADP to CPR entails entropy changes more favorable than those for binding of the same ligand to the isolated FAD-binding domain. As a consequence, the number of accessible conformational substates increases upon binding of 2′,5′-ADP to CPR. This distal effect of coenzyme binding on the energetics of the entire CPR agrees with previous temperature-jump studies reporting an increase in interdomain electron-transfer rates upon binding of 2′,5′-ADP to CPR (*11*, *12*). The global nature of this effect is further illustrated by the unforeseen finding that electron transfer from CPR ($FMN_{sq}$) to cytochrome *c* is strictly dependent on, and synchronized to, NADPH binding (Figure 8). It would hence appear that the coenzyme binding energy induces a redistribution of the conformer ensemble, populating states that are more favorable for intramolecular (FAD to FMN) and intermolecular (FMN to cytochrome *c*) electron transfer. This conclusion is reaffirmed by the observation that although two-electron reduction by dithionite results in the formation of the same redox species as reduction by NADPH (*11*), any interaction with $SO_2^-$ ion (the actual reducing species during dithionite oxidation) is incapable of reproducing the effect triggered by NADPH binding.

The existence of a complex interplay between NADPH binding and catalysis in the diflavin protein family was first suggested by studies on the P450-$BM_3$ enzyme (*13*). Subsequently, studies with CPR (*11*, *12*) and NOS enzymes (*15*) using a variety of techniques and experimental approaches reached similar conclusions. However, some uncertainty about the molecular mechanism(s) and driving force(s) behind this complex linkage remains (*16*). In particular, the suitability of midpoint redox equilibrium potential to describe the observed kinetics has been called into question (*58*). The problem of the identification of causal relations in protein-mediated electron transfer is greatly compounded by the fact that observed rates are a function of conformational and electronic parameters, not just the equilibrium potential differential ($\Delta E$) between the redox centers (*53*−*55*). Therefore, it is conceivable that electron-transfer rates could be modulated by an increase in conformational dynamics leading to high collision rates without any changes in the observed equilibrium redox potentials. Indeed, this is the case for the enhancement in interdomain electron-transfer rates in human CPR effected by 2′,5′-ADP binding (*12*). However, as shown in the seminal work by Oprian and Coon, midpoint redox potentials in CPR are by no means arbitrary (*59*). Rather, they delimit the equilibrium redox driving forces within which time-dependent electron transfer takes place (*24*, *53*, *59*).

The results presented here reveal a synchronized mechanism that is essentially dependent on coenzyme binding energy (Figure 8). This mechanism controls the molecular recognition of the redox partner, cytochrome *c*, with an apparent half-time $\tau_{50}$ of 330 ± 70 ms (Figure 8). However, it is most likely that the levels of control in CPR are multiple. This is illustrated by the finding that the affinity of the isolated FMN-binding domain for cytochrome *c* operates in a fine redox-dependent modulation that correlates with the catalytic cycle (Figure 7). This mechanism operates only when the steric constraints in the FMN-binding domain are eliminated by the propagation of coenzyme binding energy within the CPR molecule. This multiplicity of controls reflects the fact that enzymes in general appear to use a combination of strategies to achieve efficient catalysis (*60*). CPR-diflavin reductases admirably achieve this within the constraints imposed by evolutionary selection and by thermodynamic principles pertaining to a polypeptide ensemble.

## ACKNOWLEDGMENT

We thank Roland Wolf (University of Dundee) for providing the expression constructs used in these studies. We are grateful to Derek Messenger (University of Leicester) for assistance with $NADP^+$ hydrogenation experiments and Gordon Roberts (University of Leicester) and Matthew Cliff (University College London) for insightful discussions. We thank Nigel Scrutton (University of Leicester) for facilitating access to anaerobic stopped-flow instrumentation. We thank Jonathan Taylor (University College London) for help in making Figure 1.

## REFERENCES

1. Sem, D. S., and Kasper, C. B. (1994) Kinetic mechanism for the model reaction of NADPH-cytochrome P450 oxidoreductase with cytochrome *c*, *Biochemistry 33*, 12012−12021.
2. Enoch, H. G., and Strittmatter, P. (1979) Cytochrome b5 reduction by NADPH-cytochrome P-450 reductase, *J. Biol. Chem. 254*, 8976−8981.
3. Schacter, B. A., Nelson, E. B., Marver, H. S., and Masters, B. S. (1972) Immunochemical evidence for an association of heme oxygenase with the microsomal electron transport system, *J. Biol. Chem. 247*, 3601−3607.
4. Ilan, Z., Ilan, R., and Cinti, D. L. (1981) Evidence for a new physiological role of hepatic NADPH:ferricytochrome (P-450) oxidoreductase. Direct electron input to the microsomal fatty acid chain elongation system, *J. Biol. Chem. 256*, 10066−10072.
5. Bailey, S. M., Lewis, A. D., Patterson, L. H., Fisher, G. R., Knox, R. J., and Workman, P. (2001) Involvement of NADPH:cytochrome P450 reductase in the activation of indoloquinone EO9 to free radical and DNA damaging species, *Biochem. Pharmacol. 62*, 461−468.
6. Saunders, M. P., Jaffar, M., Patterson, A. V., Nolan, J., Naylor, M. A., Phillips, R. M., Harris, A. L., and Stratford, I. J. (2000) The relative importance of NADPH:cytochrome *c* (P450) reductase for determining the sensitivity of human tumour cells to the indolequinone EO9 and related analogues lacking functionality at the C-2 and C-3 positions, *Biochem. Pharmacol. 59*, 993−996.

7. Jaffar, M., Williams, K. J., and Stratford, I. J. (2001) Bioreductive and gene therapy approaches to hypoxic diseases, *Adv. Drug Delivery Rev. 53*, 217−228.
8. Rooseboom, M., Commandeur, J. N., and Vermeulen, N. P. (2004) Enzyme-catalyzed activation of anticancer prodrugs, *Pharmacol. Rev. 56*, 53−102.
9. Porter, T. D., and Kasper, C. B. (1986) NADPH-cytochrome P-450 oxidoreductase: Flavin mononucleotide and flavin adenine dinucleotide domains evolved from different flavoproteins, *Biochemistry 25*, 1682−1687.
10. Gutierrez, A., Grunau, A., Paine, M., Munro, A. W., Wolf, C. R., Roberts, G. C., and Scrutton, N. S. (2003) Electron transfer in human cytochrome P450 reductase, *Biochem. Soc. Trans. 31*, 497−501.
11. Gutierrez, A., Paine, M., Wolf, C. R., Scrutton, N. S., and Roberts, G. C. (2002) Relaxation kinetics of cytochrome P450 reductase: Internal electron transfer is limited by conformational change and regulated by coenzyme binding, *Biochemistry 41*, 4626−4637.
12. Gutierrez, A., Munro, A. W., Grunau, A., Wolf, C. R., Scrutton, N. S., and Roberts, G. C. (2003) Interflavin electron transfer in human cytochrome P450 reductase is enhanced by coenzyme binding. Relaxation kinetic studies with coenzyme analogues, *Eur. J. Biochem. 270*, 2612−2621.
13. Murataliev, M., Klein, M., Fulco, A., and Feyeresien, R. (1997) Functional interactions in cytochrome P450BM3: Flavin semiquinone intermediates, role of NADP(H), and mechanism of electron transfer by the flavoprotein domain, *Biochemistry 36*, 8401−8412.
14. Murataliev, M. B., and Feyereisen, R. (2000) Interaction of NADP(H) with oxidized and reduced P450 reductase during catalysis. Studies with nucleotide analogues, *Biochemistry 39*, 5066−5074.
15. Craig, H. D., Chapman, S. K., and Daff, S. (2002) Calmodulin activates electron transfer through neuronal nitric-oxide synthase reductase domain by releasing an NADPH-dependent conformational lock, *J. Biol. Chem. 277*, 33987−33994.
16. Murataliev, M. B., Feyereisen, R., and Walker, F. A. (2004) Electron transfer by diflavin reductases, *Biochim. Biophys. Acta 1698*, 1−26.
17. Dill, K., and Bromberg, S. (2003) *Molecular driving forces*, Garland Science, London.
18. Smith, G. C., Tew, D. G., and Wolf, C. R. (1994) Dissection of NADPH-cytochrome P450 oxidoreductase into distinct functional domains, *Proc. Natl. Acad. Sci. U.S.A. 91*, 8710−8714.
19. Gutierrez, A., Lian, L.-Y., Wolf, C. R., Scrutton, N. S., and Roberts, G. C. (2001) Stopped-flow kinetic studies of flavin reduction in human cytochrome P450 reductase and its component domains, *Biochemistry 40*, 1964−1975.
20. Fisher, H. F., and Singh, N. (1995) Calorimetric methods for interpreting protein−ligands interactions, *Methods Enzymol. 259*, 194−221.
21. Wiseman, T., Williston, S., Brandts, J. F., and Lin, L. N. (1989) Rapid measurement of binding constants and heats of binding using a new titration calorimeter, *Anal. Biochem. 179*, 131−137.
22. Ellis, K. J., and Morrison, J. F. (1982) Buffers of constant ionic strength for studying pH-dependent processes, *Methods Enzymol. 87*, 405−426.
23. Bielmann, J.-F., and Jung, M. J. (1971) Mechanism of alcohol dehydrogenases from yeast and horse liver, *Eur. J. Biochem. 19*, 130−134.
24. Munro, A. W., Noble, M. A., Robledo, L., Daff, S. N., and Chapman, S. K. (2001) Determination of the redox properties of human NADPH-cytochrome P450 reductase, *Biochemistry 40*, 1956−1963.
25. Pettigrew, G. W., and Moore, G. R (1987) *Cytochromes c. Biological aspects*, pp 83−84, Springer-Verlag, Berlin.
26. Deng, Z., Aliverti, A., Zanetti, G., Arakaki, A. K., Ottado, J., Orellano, E. G., Calcaterra, N. B., Ceccarelli, E. A., Carrillo, N., and Karplus, P. A. (1999) A productive $NADP^+$ binding mode of ferredoxin-$NADP^+$ reductase revealed by protein engineering and crystallographic studies, *Nat. Struct. Biol. 6*, 847−853.
27. Piubelli, L., Aliverti, A., Arakaki, A. K., Carrillo, N., Ceccarelli, E. A., Karplus, P. A., and Zanetti, G. (2000) Competition between C-terminal tyrosine and nicotinamide modulates pyridine nucleotide affinity and specificity in plant ferredoxin-$NADP^+$ reductase, *J. Biol. Chem. 275*, 10472−10476.
28. Roitel, O., Scrutton, N. S., and Munro, A. W. (2003) Electron transfer in flavocytochrome P450BM3: Kinetics of flavin reduction and oxidation, the role of cysteine 999, and relationships with mammalian cytochrome P450 reductase, *Biochemistry 42*, 10809−10821.
29. Lakowicz, J. R. (1999) *Principles of Fluorescence Spectroscopy*, 2nd ed., Chapter 3, pp 63−65, Kluwer Academic/Plenum Publishers: New York.
30. Wang, M., Roberts, D. L., Paschke, R., Shea, T. M., Masters, B. S., and Kim, J. J. (1997) Three-dimensional structure of NADPH-cytochrome P450 reductase: Prototype for FMN- and FAD-containing enzymes, *Proc. Natl. Acad. Sci. U.S.A. 94*, 8411−8416.
31. Sturtevant, J. M. (1977) Heat capacity and entropy changes in processes involving proteins, *Proc. Natl. Acad. Sci. U.S.A. 74*, 2236−2240.
32. Luque, I., Todd, M. J., Gomez, J., Semo, N., and Freire, E. (1998) Molecular basis of resistance to HIV-1 protease inhibition: A plausible hypothesis, *Biochemistry 37*, 5791−5797.
33. Spolar, R. S., and Record, M. T., Jr. (1994) Coupling of local folding to site-specific binding of proteins to DNA, *Science 263*, 777−784.
34. Gomez, J., Hilser, V. J., Xie, D., and Freire, E. (1995) The heat capacity of proteins, *Proteins 22*, 404−412.
35. Sem, D. S., and Kasper, C. B. (1993) Enzyme−substrate binding interactions of NADPH-cytochrome P-450 oxidoreductase characterized with pH and alternate substrate/inhibitor studies, *Biochemistry 32*, 11539−11547.
36. Bastiaens, P. I., Bonants, P. J., Muller, F., and Visser, A. J. (1989) Time-resolved fluorescence spectroscopy of NADPH-cytochrome P-450 reductase: Demonstration of energy transfer between the two prosthetic groups, *Biochemistry 28*, 8416−8425.
37. Bergqvist, S., Williams, M. A., O'Brien, R., and Ladbury, J. E. (2004) Heat capacity effects of water molecules and ions at a protein-DNA interface, *J. Mol. Biol. 336*, 829−842.
38. Gutierrez, A., Doehr, O., Paine, M., Wolf, C. R., Scrutton, N. S., and Roberts, G. C. (2000) Trp-676 facilitates nicotinamide coenzyme exchange in the reductive half-reaction of human cytochrome P450 reductase: Properties of the soluble W676H and W676A mutant reductases, *Biochemistry 39*, 15990−15999.
39. Mathews, F. S., Mauk, A. G., and Moore, G. R. (2000) Protein−protein complexes formed by electron transfer proteins. In *Protein−Protein Recognition* (Kleanthous, C., Ed.) Frontiers in Molecular Biology Series, Oxford Press, Oxford, U.K.
40. Koppenol, W. H., Rush, J. D., Mills, J. D., and Margoliash, E. (1991) The dipole moment of cytochrome *c*, *Mol. Biol. Evol. 8*, 545−558.
41. Zhao, Q., Modi, S., Smith, G., Paine, M., McDonagh, P. D., Wolf, C. R., Tew, D., Lian, L.-Y., Roberts, G. C., and Driessen, H. P. (1999) Crystal structure of the FMN-binding domain of human cytochrome P450 reductase at 1.93 Å resolution, *Protein Sci. 8*, 298−306.
42. Barsukov, I., Modi, S., Lian, L.-Y., Sze, K. H., Paine, M., Wolf, C. R., and Roberts, G. C. (1997) $^1H$, $^{15}N$ and $^{13}C$ NMR resonance assignment, secondary structure and global fold of the FMN-binding domain of human cytochrome P450 reductase, *J. Biol. NMR 10*, 63−75.
43. Murataliev, M. B., and Feyereisen, R. (1999) Mechanism of cytochrome P450 reductase from the housefly: Evidence for an FMN semiquinone as electron donor, *FEBS Lett. 453*, 201−204.
44. Pettigrew, G. W., Goodhew, C. F., Cooper, A., Nutley, M., Jumel, K., and Harding, S. E. (2003) The electron transfer complexes of cytochrome *c* peroxidase from *Paracoccus denitrificans*, *Biochemistry 42*, 2046−2055.
45. Nisimoto, Y. (1986) Localization of cytochrome *c*-binding domain on NADPH-cytochrome P-450 reductase, *J. Biol. Chem. 261*, 14232−14239.
46. Nisimoto, Y., and Otsuka-Murakami, H (1988) Cytochrome $b_5$, cytochrome *c*, and cytochrome P450 interactions with NADPH-cytochrome P450 reductase in phospholipids vesicles, *Biochemistry 27*, 5869−5876.
47. Medina, M., Luquita, A., Tejero, J., Hermoso, J., Mayoral, T., Sanz-Aparicio, J., Grever, K., and Gómez-Moreno, C. (2001) Probing the determinants of coenzyme specificity in ferredoxin-$NADP^+$ reductase by site-directed mutagenesis, *J. Biol. Chem. 276*, 11902−11912.
48. Knight, K., and Scrutton, N. S. (2002) Stopped-flow kinetic studies of electron transfer in the reductase domain of neuronal nitric oxide synthase: Re-evaluation of the kinetic mechanism reveals new

enzyme intermediates and variation with cytochrome P450 reductase, *Biochem. J. 367*, 19−30.
49. McLean, K. J., Scrutton, N. S., and Munro, A. W. (2003) Kinetic, spectroscopic and thermodynamic characterization of the *Mycobacterium tuberculosis* adrenodoxin reductase homologue FprA, *Biochem. J. 372*, 317−327.
50. Hubbard, P. A., Shen, A. L., Paschke, R., Kasper, C. B., and Kim, J. J. (2001) NADPH-cytochrome P450 oxidoreductase. Structural basis for hydride and electron transfer, *J. Biol. Chem. 276*, 29163−29170.
51. Zhang, J., Martasek, P., Paschke, R., Shea, T., Siler Masters, B. S., and Kim, J. J. (2001) Crystal structure of the FAD/NADPH-binding domain of rat neuronal nitric-oxide synthase. Comparisons with NADPH-cytochrome P450 oxidoreductase, *J. Biol. Chem. 276*, 37506−37513.
52. Daff, S. (2004) An appraisal of multiple NADPH binding-site models proposed for cytochrome P450 reductase, NO synthase, and related diflavin reductase systems, *Biochemistry 43*, 3929−3932.
53. Page, C. C., Moser, C. C., and Dutton, P. L. (2003) Mechanism for electron transfer within and between proteins, *Curr. Opin. Chem. Biol. 7*, 551−556.
54. Leys, D., Basran, J., Talfournier, F., Sutcliffe, M. J., and Scrutton, N. S. (2003) Extensive conformational sampling in a ternary electron-transfer complex, *Nat. Struct. Biol. 10*, 219−225.
55. Liang, Z. X., Nocek, J. M., Huang, K., Hayes, R. T., Kurnikov, I. V., Beratan, D. N., and Hoffman, B. M. (2002) Dynamic docking and electron transfer between Zn-myoglobin and cytochrome $b_5$, *J. Am. Chem. Soc. 124*, 6849−6859.
56. Shen, A. L., and Kasper, C. B. (1995) Role of Acidic Residues in the Interaction of NADPH-Cytochrome P450 Oxidoreductase with Cytochrome P450 and Cytochrome *c*, *J. Biol. Chem. 270*, 27475−27480.
57. Hall, D. A., Vander Kooi, C. W., Stasik, C. N., Stevens, S. Y., Zuiderweg, E. R. P., and Matthews, R. G. (2001) Mapping the interactions between flavodoxin and its physiological partners flavodoxin reductase and cobalamin-dependent methionine synthase, *Proc. Natl. Acad. Sci. U.S.A. 98*, 9521−9526.
58. Murataliev, M. B., and Feyereisen, R. (2000) Functional interactions in cytochrome $P450_{BM3}$. Evidence that NADP(H) binding controls redox potentials of the flavin cofactors, *Biochemistry 39*, 12699−12707.
59. Oprian, D. D., and Coon, M. J. (1982) Oxidation−reduction states of FMN and FAD in NADPH-cytochrome P-450 reductase during reduction by NADPH, *J. Biol. Chem. 257*, 8935−8944.
60. Kraut, D. A., Carroll, K. S., and Herschlag, D. (2003) Challenges in enzyme mechanism and energetics, *Annu. Rev. Biochem. 72*, 517−571.

BI052115R